G-1-04

Extended Abstracts of the 2018 International Conference on Solid State Devices and Materials, Tokyo, 2018, pp449-450

Electromigration Behavior of Cu/SiCN to Cu/SiCN Hybrid Bonds for 3D Integrated Circuits

Joke De Messemaeker, Soon-Wook Kim, Michele Stucchi, Gerald Beyer, Eric Beyne and Kristof Croes

[1] imec
Kapeldreef 75, 3001 Leuven, Belgium
Phone: +32-16-28-1743 E-mail: joke.demessemaeker@imec.be

Abstract

Cu/SiCN to Cu/SiCN hybrid bonds (540 nm top pad to 1620 nm bottom pad) were tested in electromigration. For electrons flowing up, failure occurred in the top current feed line, and a lower bound j_{max} at 100 °C of 8.9 MA/cm² is estimated for the top pad (i.e. an I_{max} of 25 mA per pad-to-pad connection). For electrons flowing down, a different electromigration mechanism is observed, where the gap and void volume present at the bonding interface collect and move up to the top of the top pad along the TaNTa/Cu interface at the pad sidewall. This calls for a fundamental understanding of void agglomeration in hybrid bonds due to electric current, and for a quantification of their impact on electromigration.

1. Introduction

Wafer-to-wafer hybrid bonding of patterned copper-dielectric surfaces is one of the key technologies that enable submicron pitch scaling in 3D IC integration. Recently we demonstrated how our processing approach based on unequal top and bottom pad sizes, optimized CMP for Cu protrusion (top) and Cu recess (bottom), and use of low temperature SiCN-to-SiCN dielectric, allows scaling below 2 μm pitch [1].

Electromigration (EM) tests on 3.6 μm wide hybrid bonded Cu pads were reported not to fail in the pads, as the back-end-of-line (BEOL) metal interconnect proved to be the weakest point [2]. This work reports on EM tests performed on much smaller 540 nm wide top pads bonded to 1620 nm wide bottom pads, with a pitch of 3240 nm, using a dedicated EM test structure with wide current feed lines.

2. Samples and test approach

Processing

Wafers with a single BEOL layer were processed at imec in our hybrid wafer-to-wafer bonding integration scheme implemented on a 300 mm via-middle TSV wafer platform (details described in [1]). The pad layer processing on top of the single BEOL layer consists of dielectric deposition and CMP, pad etch, 6 nm TaNTa barrier deposition, pad fill and pad CMP. The pad CMP process was tuned such that the smaller top pads are protruding and the larger bottom pads are recessed. Pad thickness after CMP is ~ 600 nm.

Test structure

The EM test structure consists of a bonded pad pair (540 nm top, 1620 nm bottom) in the center of a 5x5 dummy pad array (Fig. 1). Wide lines feed the current to the pads from 2 sides to reduce current crowding. The angle of 90° between top and bottom feed lines further promotes a good spread of the current density over the pads.

Electromigration tests

In one group of EM tests the electron flow was sent up (“e-flow up”), while in another the electrons were sent down (“e-flow down”, Fig. 1b). The test current density in the top pad j_{TOP} was 13.7 MA/cm², and the test temperature T was 240 °C. In addition, e-flow up tests were done where either j_{TOP} was lowered to 8.2 MA/cm², or T was lowered to 200 °C. Test temperatures were corrected for Joule heating (12 or 20 °C depending on j_{TOP}).

From the resistance change recorded during the test, a time to failure was extracted at 20 % resistance increase.

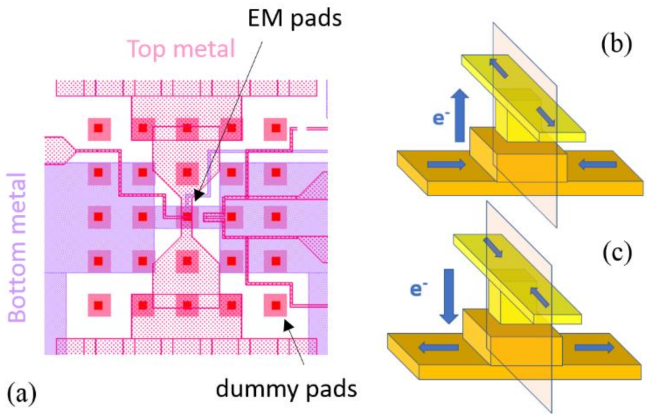

Fig. 1 EM test structure. (a) Top-down layout view with dummy pads; (b-c) 3D view of EM pads and current feed lines for e-flow up and down resp., and the plane of cross section for failure analysis.

3. Results and discussion

Tests with electron flow up

Fig. 2a shows the distribution of the time to failure for the 3 tests with electrons flowing up. These were fit to a lognormal distribution and Black’s equation [3], resulting in an activation energy E_a = 0.93 eV and current exponent n = 1.9. The scale parameter of the lognormal distribution is σ = 0.53.

The EM pads were sectioned with a FIB after the test, showing void formation and failure occurring in the top metal Fig. 3). This is due to the electron wind through the top metal, carrying Cu atoms away from the top pad in 2 directions, until a critical vacancy concentration is reached and a void is nucleated and subsequently grows. Smaller voids are visible at the bonding interface, but these are also present in the thermal reference and therefore no result of the current.

As the failure does not occur in the pads, and lifetime is limited by the EM performance of the top metal, we can only calculate a lower bound to the EM performance of the pads. Using Black's equation and the obtained EM parameters, the lower bound maximum allowable current density in the 540 nm top pads j_{max}, to have less than 0.01 % failures in 10 years at an operating temperature of 100 °C, is 8.9 MA/cm².

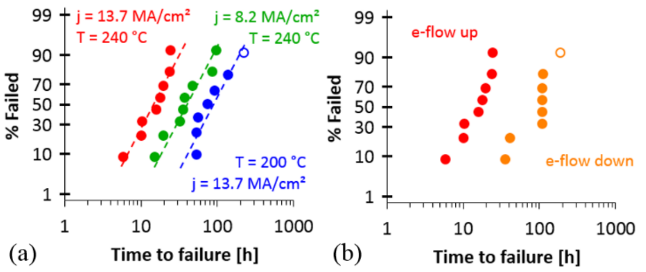

Fig. 2 Lognormal probability plot of time to failure for (a) e-flow up, different temperature and current conditions; (b) T = 240 °C & j_{TOP} = 13.7 MA/cm², e-flow up and down. Open markers represent tests stopped before failure.

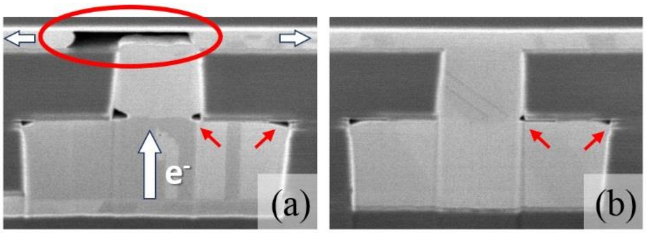

Fig. 3: Cross section after failure for a sample tested with electron flow up (T = 200 °C – j_{TOP} = 13.7 MA/cm²). (a) EM pads; (b) thermal reference.

Tests with electron flow down

The distribution of the time to failure for the test with electrons flowing up is shown in Fig. 2b. The lifetime of the samples is significantly increased relative to the e-flow up test with the same temperature and current stress, due to the wider bottom metal line. Cross sections of the EM pads after failure show voiding in the bottom metal line, analogous to the voiding in the top metal line for the e-flow up tests, and a large void at the top of the top pad (Fig. 4a). Comparison with the thermal reference indicates that Cu atoms driven down through the pads by the electron wind are filling the gaps and voids remaining at the pad interface after bonding. Concurrently the 'empty' volume from these gaps and voids is displaced in the direction opposite the electron flow, and collected at the top of the top pad. Consecutive sections of a tested sample which had not yet failed, reveal how the gaps and voids originally at the bonding interface are collected in a large void, moving up along the back sidewall of the top pad (Fig. 4b). This suggests that in EM the empty volume behaves as a pre-existing void moving up along the TaNTa barrier/Cu interface at the sidewall(s) of the top pad, and will become a dominant contributor to EM failures in extremely scaled hybrid pad-to-pad connections. This observation has a high impact and calls for a fundamental understanding of the observed void agglomeration, and for a quantification of the impact of existing voids on electromigration.

Further tests with lower temperature and current are ongoing to estimate the EM parameters and a j_{max} value corresponding to this pad failure mechanism.

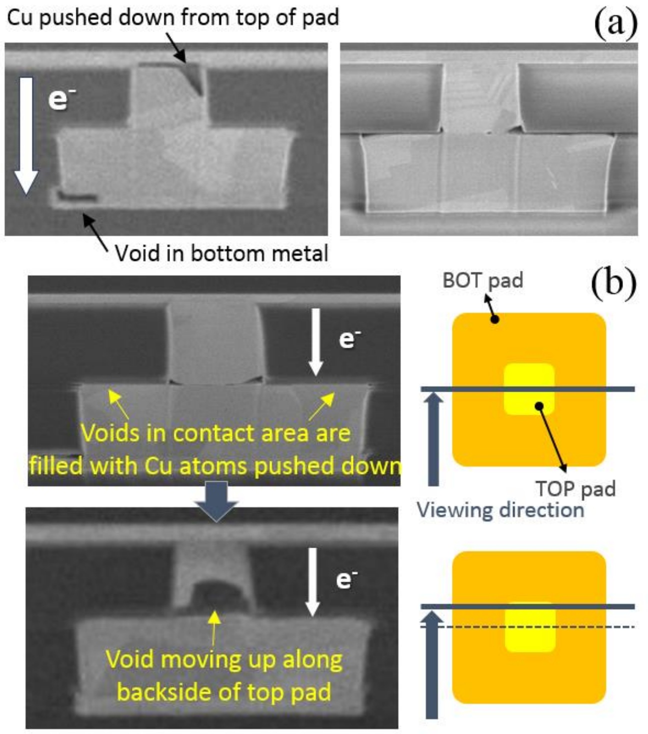

Fig. 4: (a) Cross section after failure for a sample tested with electron flow down (T = 240 °C – j_{TOP} = 13.7 MA/cm²); EM pads (left) and thermal reference (right). (b) Consecutive sections of EM pads in a sample before failure, from the test with electron flow down.

3. Conclusions

A new electromigration mechanism for hybrid bonding pads was identified, where under influence of the electron wind, gaps and voids at the bonding interface collect in a void which moves up along the Cu/barrier interface at the pad sidewall, opposite to the electron flow direction. This has the significant consequence that gaps and voids at the bonding interface will be dominant contributors to electromigration failures in extremely scaled hybrid pad-to-pad connections.

A lower bound j_{max} of 8.9 MA/cm² at 100 °C for the top pad, or a maximum current of 25 mA per pad-to-pad connection was estimated (10 y, < 0.01 % failures).

Acknowledgements

This work was supported by the IIAP of imec and the combined efforts of the 3D team at imec, and its partners.

References

[1] E. Beyne et al., *63rd International Electron Devices Meeting* (2017) 32.4.1.

[2] L. Arnaud et al., *International Reliability Physics Symposium* (2018) 4D.4-1.

[3] J.R. Black, Trans. El. Devices **16** (1969) 338.